10-20-2020

Tadpole of the Amazonia frog Edalorhina perezi (Anura: Leptodactylidae) with description of oral internal and chondrocranial morphology

Filipe A.C do Nascimento

Rafael O. de Sá
University of Richmond, rdesa@richmond.edu

Paulo C. de A. Garcia

Recommended Citation

do Nascimento, F. A. C., de Sá, R.O., and Garcia, P. C. de A. 2020. Tadpole of the Amazonian frog Edalorhina perezi (Anura: Leptodactylidae) with description of oral internal and chondrocranial morphology. Journal of Morphology: 1–12; https://doi.org/10.1002/jmor.21286.

Received: 31 January 2020 | Revised: 24 March 2020 | Accepted: 6 October 2020

DOI: 10.1002/jmor.21286

RESEARCH ARTICLE

JOURNAL OF morphology WILEY

Tadpole of the Amazonia frog *Edalorhina perezi* (Anura: Leptodactylidae) with description of oral internal and chondrocranial morphology

Filipe A. C. do Nascimento[1,2] | **Rafael O. de Sá**[3] | **Paulo C. de A. Garcia**[2,4]

[1]Setor de Herpetologia, Museu de História Natural, Universidade Federal de Alagoas, Maceió, Alagoas, Brazil

[2]Pós-Graduação em Zoologia, Instituto de Ciências Biológicas, Universidade Federal de Minas Gerais, Belo Horizonte, Minas Gerais, Brazil

[3]Department of Biology, University of Richmond, Richmond, Virginia

[4]Departamento de Zoologia, Instituto de Ciências Biológicas, Universidade Federal de Minas Gerais, Belo Horizonte, Minas Gerais, Brazil

Correspondence
Filipe A. C. do Nascimento, Setor de Herpetologia, Museu de História Natural, Universidade Federal de Alagoas, Maceió, Alagoas, Brazil.
Email: filipe.nascimento@mhn.ufal.br

Funding information
Coordenação de Aperfeiçoamento de Pessoal de Nível Superior - Brasil (CAPES), Grant/Award Number: Code 001

Abstract

The genus *Edalorhina* consists of two species of small forest-floor frogs inhabiting the Amazon basin. The tadpole of *Edalorhina perezi*, the most widely distributed species, was previously described based on a single and early stage (Gosner 25) individual. Herein, we provide a description of the tadpole in Gosner stages 35–36 including internal morphology data (i.e., buccopharyngeal cavity and larval skeleton) based on samples from two populations from Ecuador. *Edalorhina* shares a generalized morphology with most members of its closely related taxa; however, it is distinguished from the other species by having an almost terminal oral disc. The presence of a dextral vent tube is considered a synapomorphy for the clade consisting of *Edalorhina*, *Engystomops*, and *Physalaemus*. Within this clade, the combination of two lingual papillae, a filiform median ridge, and the lack of buccal roof papillae are diagnostic of *E. perezi* and putative autapomorphies of *Edalorhina*. Chondrocranial anatomy provides characteristics, that is, presence of and uniquely shaped *processus pseudopterygoideus* and *cartilago suprarostralis* with corpora and alae joined by dorsal and ventral connections that readily differentiates the genus from other Leiuperinae.

KEYWORDS
larval SEM, Leiuperinae, systematics

1 | INTRODUCTION

The genus *Edalorhina* consists of two described species of small forest-floor frogs inhabiting the Amazon basin: *Edalorhina perezi* and *Edalorhina nasuta*. *E. perezi* is widely distributed, occurring in Ecuador and Peru, between 200 m and 1,100 m on the eastern Andes slopes, extreme southern Colombia, and surrounding areas of Brazil (Duellman & Morales, 1990; Frost, 2019), whereas *E. nasuta* is currently known from the Departments of Pasco and Huanuco in Peru (Dunn, 1949). *Edalorhina perezi* is a foam-nest builder that lays eggs on lentic water bodies (Duellman & Morales, 1990; Schlüter, 1990). The species was reported to be diurnal and the males call solitarily with no aggregations of breeding individuals (Aichinger, 1987; Duellman & Morales, 1990; Schlüter, 1990).

A close relationship of *Edalorhina* with *Physalaemus* and *Engystomops* was recovered in recent phylogenetic analyses; however, relationships can vary depending of the method employed on the same data set. *Edalorhina* was recovered closely related to *Engystomops* in parsimony analyses whereas in Bayesian analyses *Edalorhina* was the sister group to the clade consisting of *Physalaemus* and *Engystomops* (Faivovich et al., 2012; Jetz & Pyron, 2018; Lourenço et al., 2015; Pyron & Wiens, 2011; Veiga-Menoncello et al., 2014). These three genera, together with *Pleurodema* and *Pseudopaludicola* are placed in the subfamily Leiuperinae (Pyron & Wiens, 2011; Figure 1).

Leiuperinae has complex and diverse life history modes. Most species build foam-nests to reproduce; however, *Pseudopaludicola* and some species of *Pleurodema* do not (Barrio, 1954; Faivovich et al., 2012; Giaretta & Facure, 2009; Weigandt, Úbeda, & Díaz, 2004). These reproductive patterns are usually associated with a peculiar larval diversity (Kolenc, Borteiro, Baldo, Ferraro, & Prigioni, 2009; Ruggeri & Weber, 2012; Vera Candioti et al., 2011).

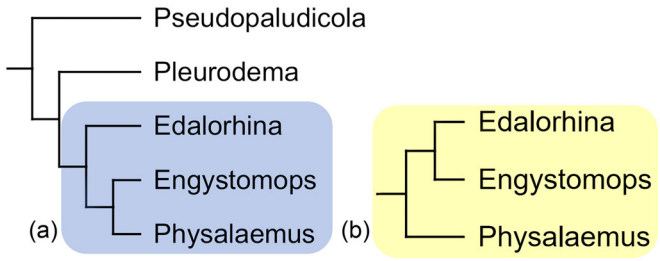

FIGURE 1 (a) Topological summary at generic level of current phylogenetic relationships of the subfamily Leiuperinae (sensu Pyron & Wiens, 2011; Lourenço et al., 2015; Jetz & Pyron, 2018), highlighting the subclade formed by *Edalorhina*, *Engystomops*, and *Physalaemus*, (b) alternative topology of this subclade (sensu Faivovich et al., 2012, Lourenço et al., 2015, Veiga-Menoncello et al., 2014)

Furthermore, tadpole morphology of this subfamily may also correlate with phylogenetic arrangements (e.g., the *Physalaemus biligonigerus* group, Lourenço et al., 2015; a subset of the *Pleurodema thaul* clade, Barrasso, Cotichelli, Alcalde, & Basso, 2013), and variation in larval morphology was reported even among closely related species (e.g., *Engystomops guayaco* and *E. petersi*; Ron, Coloma, & Cannatella, 2005).

Morphology of *Edalorhina perezi* tadpoles is poorly known; with only a brief description of its external morphology from populations in Peru (Schlüter, 1990). Herein, we provide a detailed and full description of the tadpole of *E. perezi*, including its internal oral morphology and chondrocranial anatomy. Furthermore, we compare the data for *E. perezi* with available data for the closely related genera *Physalaemus* and *Engystomops* and with other Leiuperinae.

2 | MATERIAL AND METHODS

We analyzed samples from two populations of *E. perezi* Jiménez de la Espada, 1871 tadpoles from Ecuador. Specimens are stored at the Museo de Zoología de la Pontificia Universidad Católica del Ecuador (QCAZ). The first lot (QCAZ 19141, n = 10) was collected in the Parque Nacional Yasuní, Orellana Province (01°06′S, 75°48′W; datum WGS84), and the second lot (QCAZ 37853, n = 5) came from Campo Villano, Pastaza Province (01°30′S, 77°48′W; datum WGS84). Tadpoles identity was confirmed by raising tadpoles through metamorphosis. Additionally, we included a single larval skeleton of *E. perezi* from Manu National Park, Madre de Dios Province, Peru (12°02′S, 71°43′W; datum WGS84), stored at National Museum of Natural History, Smithsonian Institution (USNM 342752).

Measurements and analysis of external morphology were based on 15 tadpoles (stages 31 to 39; following Gosner, 1960). Larval description was based on three tadpoles at stages 35–36 (QCAZ 19141). The following measurements were taking: body length (BL), maximum tail height (MTH), tail length (TaL), tail muscle height (TMH), tail muscle width (TMW), and total length (TL) (sensu Altig & McDiarmid, 1999a); body width at eye level (BWE), body width at nostril level (BWN), width of the dorsal gap of the oral disc (DGO), extranarial distance (EnD), extraorbital distance (EoD), eye diameter (ED), eye-nostril distance (END), intranarial distance (InD), intraorbital distance (IoD), maximum body height (MBH), maximum body width (MBW), narial diameter (ND), oral disc width (ODW), snout-nostril distance (SND), snout-spiracle distance (SSD), and spiracle-posterior body distance (SPD) (sensu Lavilla & Scrocchi, 1986); and dorsal fin height (DFH) and ventral fin height (VFH) (sensu Grosjean, 2005). In addition, we also included the dorsal fin insertion angle (DFIA, follows Pinheiro, Pezzuti, & Garcia, 2012) and the oral disc angular orientation (ODAO, follows Altig & Johnston, 1989). All measurements were taken using an ocular micrometer installed on a Leica® MZ6 stereomicroscope, except for TL which was measured with digital calipers (0.1 mm accuracy) and DFIA and ODAO which were measured with the aid of the ImageJ v.1.50i software (Rasband, 1997-2018) from photos taken using a digital camera installed on a Coleman® NSZ 405 stereomicroscope. Multifocal photographs were taken with a Leica M205 stereomicroscope and used for illustrations. Some tadpole structures (e.g., oral disc, vent tube, and spiracle) were stained with methylene blue solution (2%) to enhance contrast. Terminology of external morphology follows Altig and McDiarmid (1999a). Measurement given in text correspond to range, also see Tables S1–S3. Coloration description and terminology follows Kohler (2012).

The morphology of the buccopharyngeal cavity is described based on two tadpoles at stage 34 (QCAZ 37853). Specimens were dissected following Wassersug (1976) to separate buccal roof and floor. One specimen was processed for scanning electron microscope (SEM) as follows: three 10 min washes with 0.1 mol/L phosphate buffer, postfixed for 1 hr in a 1% solution of osmium tetroxide rt, three 10 min washes in 0.1 mol/L phosphate buffer were repeated, a 20 min wash with 1% tannic acid, three 10 min washes in 0.1 mol/L phosphate buffer again, 1 hr in a 1% solution of osmium tetroxide rt again, and three 10 min washes in distilled water. Subsequently, the samples were dehydrated using 10 min changes of the following graded ethanol series: two 35, two 50, two 70, two 85, two 95, and three 100% changes. The samples were critical point dried in CO_2, mounted on aluminum stubs, and sputter coated with 10 nm of gold/palladium. We used a Quanta 200 SEM at 15 kV to study the samples and take images. The terminology used follows Wassersug (1976, 1980).

Descriptions of the chondrocranial and hyobranchial apparatus are based on two tadpoles at stages 34 and 35 (QCAZ 19141). Specimens were cleared and double-stained for bone and cartilage following protocol of Dingerkus and Uhler (1977). Twenty measurements were taken: chondrocranium total length (CTL), chondrocranium maximum width (CMW), chondrocranium maximum height (CMH), *cornua trabeculae* length (CTrL), otic capsule length (OCL), otic capsule width (OCW), otic capsule height (OCH), *planum trabecularum* length (PTrL) and *planum trabecularum* width (PTrW) (sensu Alcalde & Rosset, 2003); *cornua trabeculae* maximum width (CTMW), *pars articularis quadrati* length (PAQL), *pars articularis quadrati* width (PAQW), *cartilago meckeli* length (CML), *cartilago meckeli* width (CMW), *cartilago infrarostralis* length (CIL), *cartilago infrarostralis* width (CIW), *cartilago meckeli* angle relative to the main body axis (CMA), and angle of *cartilago infrarostralis* relative to the main body axis (CIA)

(sensu Alcalde, Candioti, Kolenc, Borteiro, & Baldo, 2011); and *processus anterior hyalis* length (PAHL) and *processus anterolateralis hyalis* length (PAlHL) (sensu Haas, 2003). All measurements were taken using an ocular micrometer installed on a Leica® MZ6 stereomicroscope, except for MCA, IA, PAHL, and PAlHL which were measured with the aid of the ImageJ v.1.50i software (Rasband, 1997-2018) from photos taken using a digital camera installed on a Coleman® NSZ 405 stereomicroscope. Illustrations were made using a Leica MZ6 stereomicroscope with a camera-lucida attachment and later editing in Adobe Photoshop® software. Terminology follows Larson and de Sá (1998) and Cannatella (1999).

Character optimization was accomplished using the parsimony algorithm in Mesquite 3.20 (Maddison & Maddison, 2016). The coding of character from the other species of Leiuperinae we done from literature (see Discussion).

3 | RESULTS

3.1 | External morphology

Total length ranged from 27.6 to 29.7 mm (stages 35–36, n = 3). Body elliptical in dorsal and lateral views (MBW/BL = 0.63–0.66), depressed (MBH/MBW = 0.70–0.74), ventral contour of body convex at peribranchial region and flat to slightly convex on abdominal region, body wall with a constriction at level of spiracle. Body length about 45% of total length (BL/TL = 0.44–0.46), maximum body width at middle third of the body and maximum body height at posterior third. Snout truncated in dorsal view and rounded to slightly acuminate in lateral view (Figure 2a–c). Eyes located dorsally and directed dorsolateral; representing nearly 50% of intraorbital distance (ED/IoD = 0.47–0.56). Nostrils dorsal and directed dorsolateral, external opening circular, surrounded by a continuous and light marginal rim (Figure 2b); each nostril representing about 23% of intranarial distance (ND/InD = 0.20–29), 4% of maximum body width (ND/MBW = 0.04–0.05), and located closer to snout than eyes (END/SND = 1.18–1.40). Oral disc about 36% of maximum body width (ODW/MBW = 0.35–0.38), almost terminal (ODAO = 46.2°–55.0°), and laterally emarginated (Figure 2h). Labium bears a single row of marginal papillae (∼13 papillae/mm), with a wide gap on upper labium (DGO/ODW = 0.67–0.75). Papillae overall conical, elongated (i.e., length greater than basal width), with rounded tips, bases slightly offset and directed in alternating directions on lower labium. Lateral papillae on lower labium may be poorly differentiated. Few submarginal papillae (2–3) found laterally on lower labium. Labial tooth row formula (LTRF) 2(2)/3(1); length of each row: A1 = A2 > P1 = P2 > P3. P1 and P2 rows length about 90% of anterior

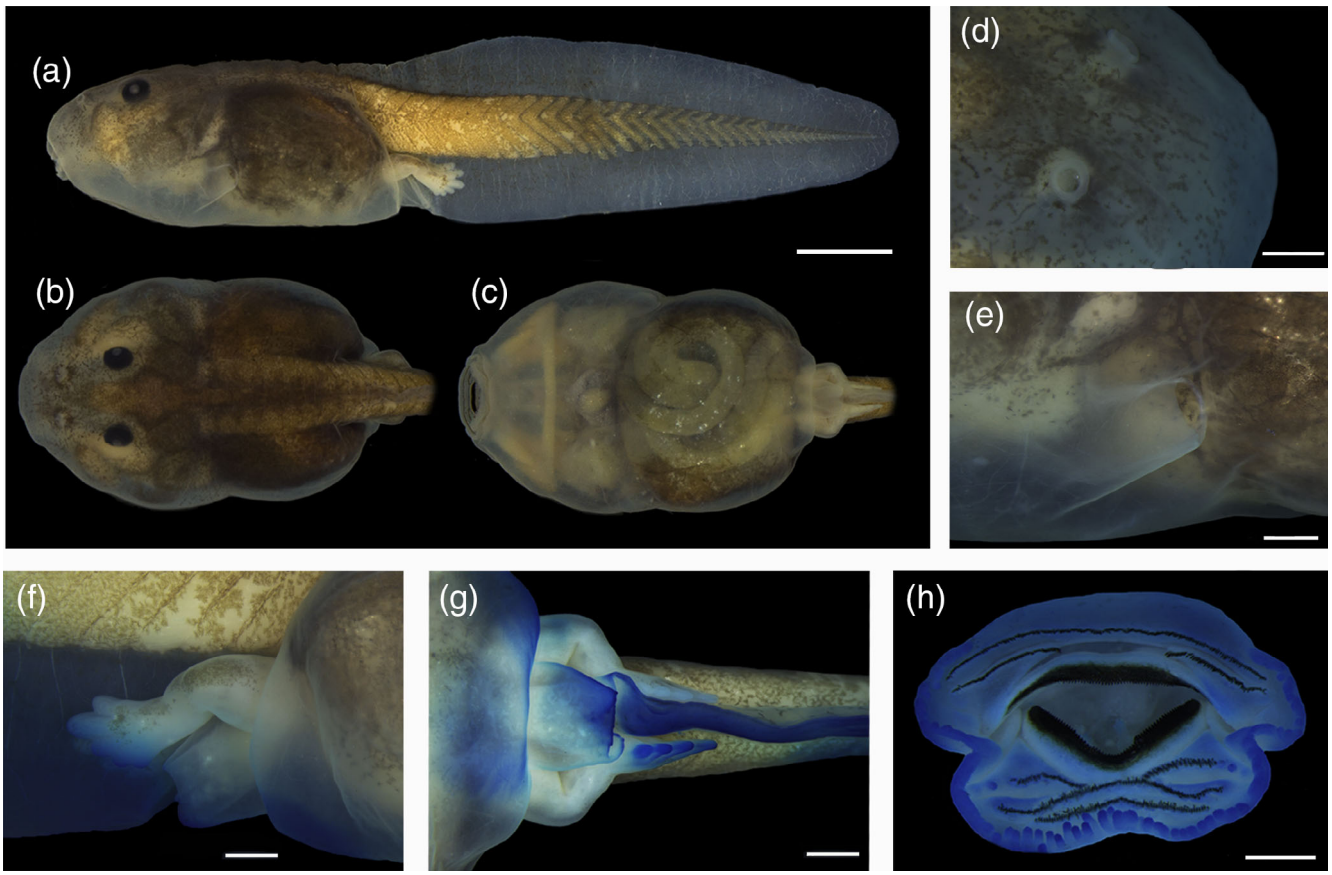

FIGURE 2 Tadpole of *Edalorhina perezi* at stage 36 (QCAZ 19141). (a) Lateral, (b) dorsal, and (c) ventral views (scale bar = 3 mm); (d) narial opening, (e) spiracle in lateral view, (f) vent tube in lateral and (g) in ventral views, and (h) oral disc (scale bar = 0.5 mm)

rows. P3 row length ~70% of other posterior rows. A2 and P1 with medial gaps (about 30% of A2 length and 10% of P1 length, respectively; Figure 3d). Jaw sheaths pigmented; upper jaw sheath arc-shaped and finely serrated (about 48 serrations/mm), serrations straight medially; lower jaw sheath broad V-shaped and finely serrated (about 45 serrations/mm), serrations dorsally oriented. Spiracle sinistral, located below body midline, opening on middle third of body (SPD/SSD = 0.64–0.70), and directed posterodorsally, forming an angle of ~25° with longitudinal body axis; inner wall present as a slight ridge (i.e., mostly fused with the body) and external wall ends anterior to insertion of inner wall (Figure 2e). Vent tube about equal in length and width, right wall displaced more dorsally and anteriorly than left wall, which is attached directly to fin margin, resulting in a large dextral opening; margin of aperture smooth (Figure 2f,g). Tail length ~55% of total length (TaL/TL = 0.54–0.55), maximum height greater than body height (MBH/MTH = 0.86–0.93), highest on first third of tail. Tail tip rounded. Tail musculature maximum height less than half of tail maximum height (TMH/MTH = 0.35–0.39), becoming progressively thinner posteriorly and extending to tail tip. Myosepta distinct anteriorly and partially visible on posterior half of tail. Dorsal fin height less than half the tail height (DFH/MTH = 0.32–0.33) and slightly lower than ventral fin (VFH/DFH = 1.05–1.09). Dorsal fin beginning at body-tail junction (DFIA = 5.39°–11.3°) with an overall convex contour; maximum height at first third of tail. Ventral fin beginning at the base of the tail, its origin concealed by vent tube and convex contour; maximum height at middle third of the tail (for measurement raw data, see Table S3).

In preservative, body dorsum and flanks coloration mostly Cinnamon Brown (43), translucent; skin with filiform/stellate shaped melanophores forming a reticulated pattern. Venter Beige (254), translucent, with no melanophores, lateral surfaces light brown suffusion. Tail musculature Cinnamon-Drab (50) densely covered with irregular shaped melanophores. Fins translucent with few dark markings forming a reticular pattern, particularly close to tail musculature.

3.1.1 | Intraspecific variation

Body shape showed subtle variations in lateral view, from elliptical to oval, as well as slight variation on arching of the fins (Figure 3a). Lot QCAZ 37853 showed some consistent differences: (a) marginal rim of the narial opening with a medially small cutaneous projection (Figure 3c); (b) vent tube with the right and left walls attached at same level, directly to fin margin; and (c) in three specimens (stages 34 and 38), the P1 labial tooth row had no gap, resulting in a LTRF 2(2)/3 (Figure 3e).

3.2 | Buccopharyngeal cavity

3.2.1 | Buccal roof

Buccal roof diamond-shaped, longer than wide (buccal roof length/width about 1.4) (Figure 4a–c). Prenarial arena wider than long (prenarial arena length/width about 0.54), with a transversal and slightly arc-shaped ridge formed by 3–4 broad papillae; ridge closer to jaw sheath than to choanae. Each papilla bears 4–8 pustules terminally. Additionally, one pustule occurs on each side and posterolateral to ridge. Choanae elongated, slight arched and slit-shaped, located about 20% the distance from jaw sheath to esophagus; maximum choanae length about 20% and internarial distance about 8% of maximum buccal roof width. Each choana oriented about 20° angle relative the

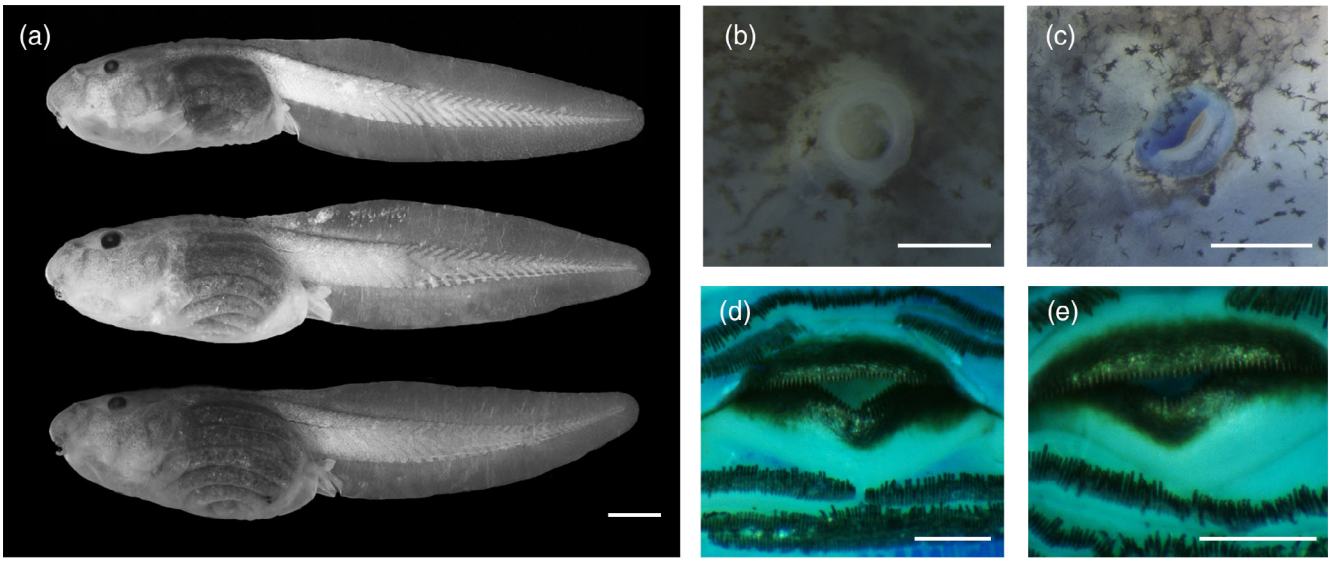

FIGURE 3 Tadpoles of *Edalorhina perezi* showing (a) the body shape and arched degree of the fins variations in lateral view (scale bar = 3 mm); (b) narial opening circular without and (c) with a medially small cutaneous projection (scale bar = 0.3 mm); (d) oral apparatus with a gap on P1 tooth row and (e) with no gap (scale bar = 0.5 mm; QCAZ 19141, 37853)

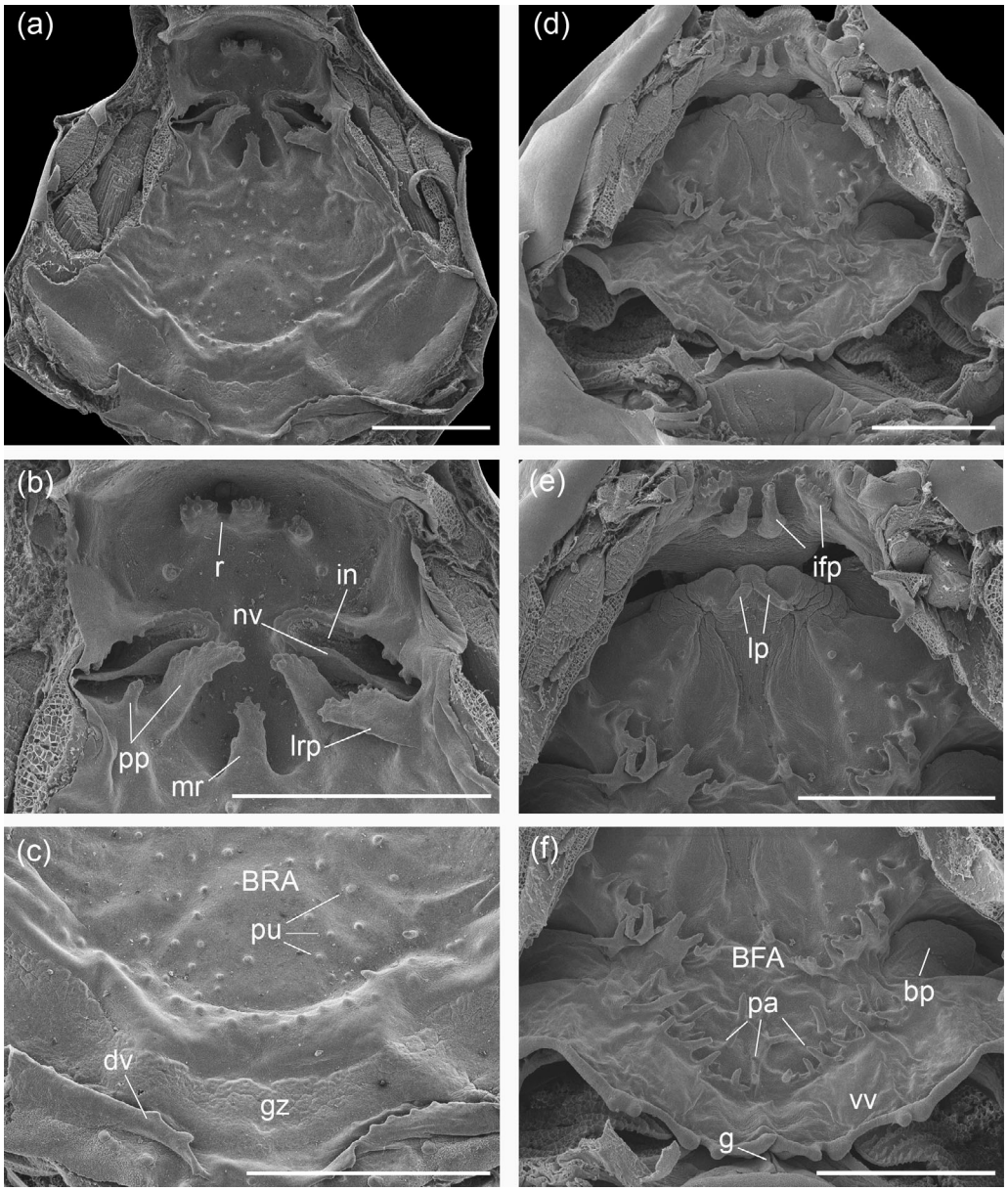

FIGURE 4 Scanning electron photomicrographs of the buccal roof (a–c) and floor (d–f) of *Edalorhina perezi* tadpole (stage 34; QCAZ 37853; scale bar = 1 mm). BFA, buccal floor arena; bp, buccal pockets; BRA, buccal roof arena; ch, choana; dv, dorsal velum; g, glottis; gz, glandular zone; ifp, infralabial papillae; lp, lingual papillae; lrp, lateral ridge papillae; mr, median ridge; nv, narial valve; pa, papillae; pp, postnarial papillae; pu, pustules; r, ridge; vv, ventral velum

transverse plane; anterior narial wall low and thin, with 15–16 pustules distributed along its length, less dense on its lateral half, which are inclined toward the narial opening. Posterior wall wider than high, with narial valve extending forward and partially overlapping the choanae. Length of postnarial arena about 85% of prenarial arena length; two pairs of postnarial papillae located close the choanae than median ridge, aligned transversally and projecting anteromedially; medial pair elongated (width/length about 0.45), bearing 8–11 pustules terminally and reaching the posterior medial wall of choanae. Postnarial papillae and medial ridge delimit a distinct concave postnarial arena; most lateral pair smaller, about 1/3 the length of medial pair, bearing 3–4 pustules terminally and concealed by lateral ridge papillae. Median ridge located about 35% of distance from jaw sheath to esophagus, filiform (width/length about 0.70), with 5–6 secondary projections on anterior surface; low papilla located far back on postnarial arena. One pair of trapezoidal (flap-like) lateral ridge papillae with 12–13 secondary projections on its anterior and medial margins, located anterolaterally to median ridge, and projecting over postnarial papillae. Buccal roof arena (BRA) diamond-shaped, delimited anteriorly by median ridge and posteriorly by about 18 pustules forming an arc-shaped ridge; no BRA papillae; 48–64 pustules distributed on the BRA, absent on its lateral ends. Glandular zone distinct, arc-shaped, medial portion narrower than lateral ones; medial portion length equivalent to 10% the buccal roof length; secretory pits distinct,

fewer laterally. Dorsal velum length equivalent to 5% the buccal roof length, interrupted medially, with 2–5 papillae on its posteromedial margin; 5–6 pustules found posterior to dorsal velum.

3.2.2 | Buccal floor

Buccal floor triangular-shaped, slightly wider than long (buccal floor length/width about 0.8) (Figure 4d–f). Two pairs of similar-sized infralabial papillae; first pair hand-shaped and located anterolaterally, with 8–12 secondary projections terminally, located almost 45° from transverse plane; second posteromedial pair stick-shaped, with 2–3 pustules terminally, located slightly ventrally to first. Approximately 15 pustules anterior to first infralabial pair, located at the level of the *cartilago infrarostralis*. Lingual anlage bears two finger-like lingual papillae with bifurcated tips. Buccal floor arena (BFA) hexagonal, with 40–58 conical BFA papillae mostly distributed in two rows, one row extends medially from the anterior region of buccal pockets to middle region of BFA, other row extends following the anterior margin of ventral velum, toward the BFA posterior region; most papillae of first row with bifurcated tips. Moreover, 5–6 papillae scattered posteriorly on BFA and 4–6 small papillae arranged obliquely forming a row on each side of anterior portion of the BFA, bordering medially by 2–4 pustules. Buccal pockets transversally oriented, width of each of them about 20% of buccal floor width, arc-shaped slits; four to five conical pre-pocket papillae. Ventral velum length equivalent to 3% of buccal roof length, posterior margin scalloped, with about six distinct small peaks over gill cavities, peaks about 6% of the buccal roof length, two to four digitiform projections medially; median notch slightly evident and projected dorsally. No secretory pits. Spicular support conspicuous; spicular length about 20% of buccal floor length. Glottis partially visible.

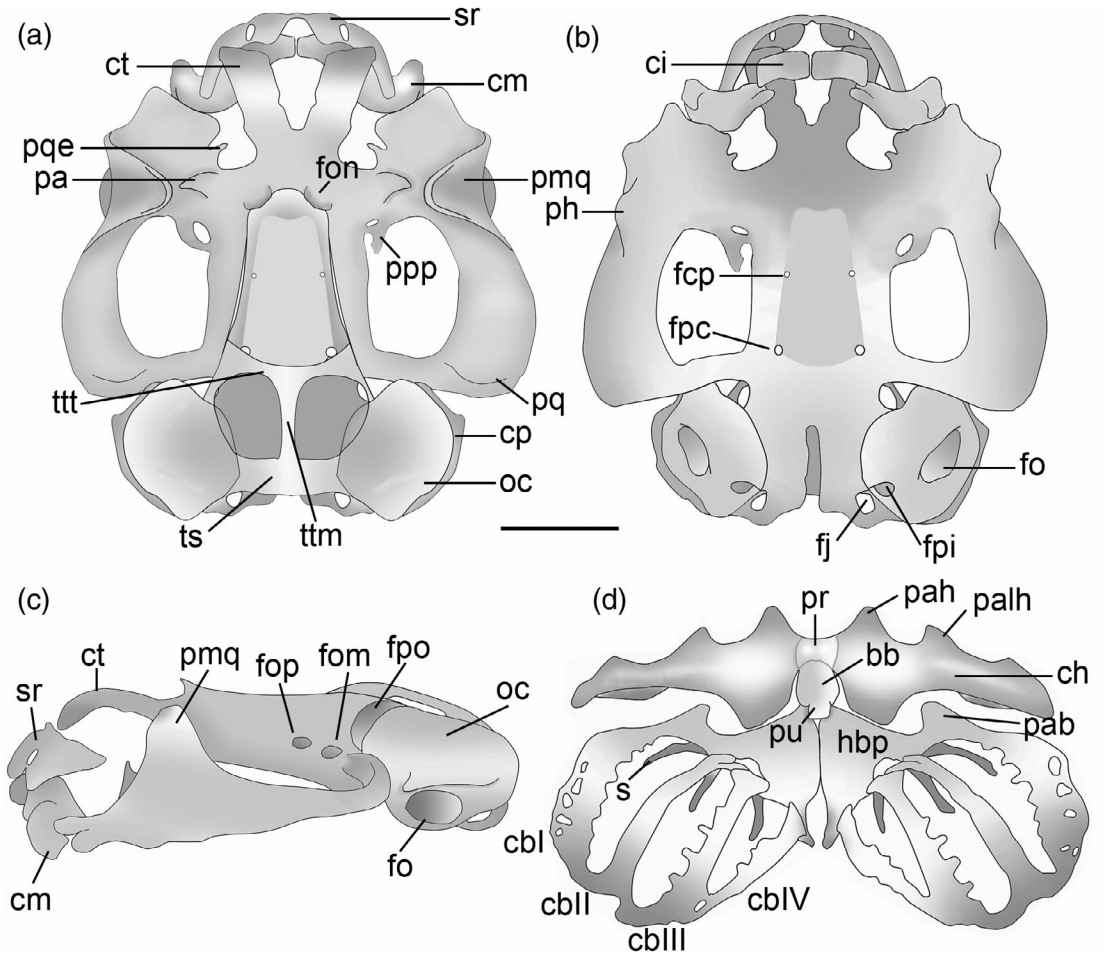

FIGURE 5 Skeleton of *Edalorhina perezi* tadpole at stage 35 (QCAZ 19141; scale bar = 5 mm). Chondrocranium in (a) dorsal, (b) ventral, and (c) lateral views; (d) hyobranchial apparatus in ventral view (scale bar = 5 mm). Bb, basihyal; cbI–cbIV, ceratobranchial I–IV; ch, *ceratohyalia*; cp, *crista parotica*; ct, *cornua trabeculae*; fcp, *foramen craniopalatinum*; fj, *foramen jugulare*; fo, *fenestra ovalis*; fom, *foramen oculomotorium*; fon, *foramen orbitonasalis*; fop, *foramen opticum*; fpc, *foramen caroticum primarium*; fpi, *foramen perilymphaticum inferior*; fpo, *foramen prooticum*; hbp, hypobranchial plate; ci, *cartilago infrarostralis*; cm, *cartilago meckeli*; oc, otic capsule; pa, *processus antorbitalis*; pab, *processus anterior branchialis*; pah, *processus anterior hyalis*; ph, processus hyoquadrati; palh, *processus anterolateralis hyalis*; pmq, *processus muscularis quadrati*; ppp, *processus pseudopterygoideus*; pq, palatoquadrate; pqe, *processus quadratoethmoidalis*; pr, *par reuniens*; pu, *processus urobranchialis*; s, spicule; sr, suprarostral cartilage; ts, *tectum sinoticum*; ttm, *taenia tecti medialis*; ttt, *taenia tecti transversalis*

3.3 | Chondrocranium and hyobranchial apparatus

Chondrocranium total length ranged from 6.0 to 6.2 mm (stages 34–35), overall ovoid in dorsal view, with equivalent length and width (CMW/CTL = 0.97–1.01), and depressed in lateral view (CMH/CMW = 0.33–0.39), highest at level of *processus muscularis quadrati* and widest at medial third of palatoquadrate (Figure 5, Table S3).

3.3.1 | Neurocranium

Ethmoidal region

Cartilago suprarostralis tetrapartite and arc-shaped in dorsal view, with corpora located between the *cornua trabeculae* at most anterior end of chondrocranium. Corpora connected ventromedially by a thin cartilage, forming a continuous V-shaped structure in frontal view. Each corpus fused to its respective lateral ala by a broad dorsolateral and a thin, ventrolateral, cartilaginous connections. Alae flat, wide, and overall triangular shaped; curving and narrowing posteriorly from the point of fusion with the corpora. Additionally, a small *processus anterior dorsalis* appears as a medial projection on dorsomedial margin of alae. No adrostral tissue mass (Figure 6a).

Cornua trabeculae extending anteriorly from *planum trabecularum anticum*, diverging distally forming a V in dorsal view and representing about 20% of total chondrocranial length (CTrL/CTL = 0.19–0.20); distal tips flexing downwards in lateral view. *Cornua* of uniform width throughout their length and anterior margin straight and syndesmotically articulated with suprarostral alae. *Processus lateralis trabeculae* evident. *Planum trabecularum anticum* wider than long (PTAW/PTAL = 1.5–2.3). *Tectum nasi* with *foramen orbitonasalis* and slight *lamina orbitonasalis*.

Orbitotemporal region

Central area of cranial floor slightly chondrified, with anterior and small *foramina craniopalatina* and posterior and larger *foramina carotica primaria* visible on cranial floor. Orbital cartilages slightly chondrified; a slight smaller *foramen opticum*, a *foramen oculomotorium*, and a largest and crescent moon shaped *foramen prooticum*, separating the otic capsule from orbital cartilage, are visible posteriorly on orbital cartilage. Frontoparietal fontanelle bell-shaped, delimited laterally by a thin *taenia tecti marginalis* and posteriorly by a *tectum synoticum*. *Tectum synoticum* length about 8% of chondrocranial length. Posterior portion of frontoparietal fontanelle with two parietal fenestrae formed by a thin and slight chondrified *taenia tecti transversalis* and *taenia tecti medialis*.

Otooccipital region

Otic capsules quadrangular (OCW/OCL = 0.75–0.91; OCH/OCW = 0.86–0.94) and ~30% of total chondrocranial length (OCL/CTL = 0.29–0.32). *Crista parotica* narrow protruding horizontally from lateral walls of otic capsules, bearing an anterior and small triangular anterolateral process; no posterolateral process. An ovoid *fenestra ovalis*, with width about 10% of chondrocranium total length, located ventrolaterally on otic capsule and below *crista parotica*. *Arcus occipitalis* extending posteromedially to otic capsules from basal plate, bearing occipital condyles and forming the medial and ventral margins of *foramen jugulare*. A slightly smaller *foramen perilymphaticum inferior* occurs on ventromedial surface of otic capsules. A notch, representing about 18% of total chondrocranial length, marks the placement of notochord within the basal plate.

3.3.2 | Visceral components

Palatoquadrate

Palatoquadrate relatively wide, expanding posteriorly, and posterolaterally curving slightly upwards to connect with orbital cartilage via *processus ascendens*. Its lateral margin is convex in dorsal view; posterolateral and posterior margin slight basket-shaped in dorsal view and extending beyond anterior margin of otic capsule. Lateral margin of subocular arc smooth. *Processus ascendens* rod-like, forming an obtuse angle relative to main body axis, curving dorsomedially, and attaching to orbital cartilage posteriorly and below the *foramen oculomotorium*. *Commissura quadratocranialis anterior* bears a triangular *processus quadratoethmoidalis* on its anterior margin, a slight chondrified, elongated, pointed, and medially curved *processus*

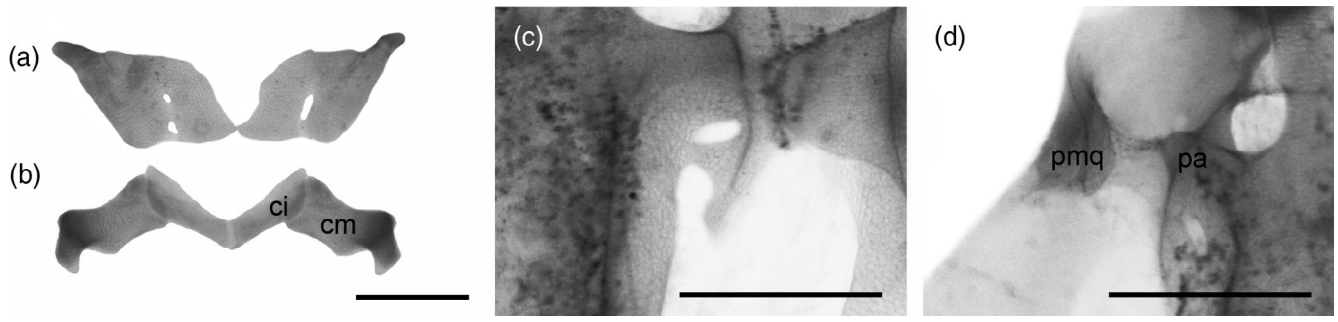

FIGURE 6 Skeleton of *Edalorhina perezi* tadpoles showing (a) the *cartilago suprarostralis* in frontal view, (b) *cartilago infrarostralis* (ci) and *cartilago meckeli* (cm) in ventral view, (c) *processus pseudopterygoideus* in dorsal view, and (d) *processus muscularis quadrati* (pmq) and *antorbitalis* (pa) in dorsal view (scale bar = 5 mm; QCAZ 19141, 37853)

pseudopterygoideus found on its posterior margin; medial margin of this process can be partially fused with orbital cartilage (Figure 6c). *Processus muscularis quadrati* broadly triangular, with its dorsal edge medially inclined and facing but not fusing with *processus antorbitalis* (*commissura quadratoorbitalis* absent; Figure 6d). *Processus hyoquadrati* subtriangular and found immediately below muscular process. *Pars articularis quadrati* usually wider than long (PAQW/PAQL = 1.0–1.5), corresponding to 10% of total chondrocranial length (PAQL/CTL = 0.10–0.12).

Cartilago meckeli and cartilago infrarostralis

Cartilago meckeli overall S-shaped in dorsal view, stout, elongated (CML/CMW = 0.42–0.44), and oriented at an almost 60° angle relative to main body axis. *Processus retroarticularis*, *dorsomedialis*, and *ventromedialis* distinct (Figure 6b). *Cartilago infrarostralis* overall wedge-shaped, connect ventromedially, forming a V-shaped structure in anterior view; wider than long (CIW/CIL = 0.48–0.50), dorsolateral margin thicker with a small notch terminally, anterior margin outwardly curved.

Hyobranchial apparatus

Ceratohyalia medially flat and oriented perpendicular to main body axis; articular process stout, extending laterodorsally from anterior margin (Figure 5d). *Processus anterior hyalis* and *processus anterolateralis hyalis* triangular, with first one larger (PAlHL/PAHL = 0.48–0.60) and last one medially inclined. *Processus posterior hyalis* triangular and well-developed. No basihyal. *Pars reuniens* rectangular and slightly chondrified. Basibranchial longer than wide, with lateral margins slightly convex and with a distinct, short, and overall squared shaped *processus urobranchialis*. Hypobranchial plates triangular-shaped, articulating synchondrostically medially; posterior borders diverging in an inverted U-shape. Branchial baskets formed by four ceratobranchials, with a few lateral projections that are distally joined by terminal commissurae. Ceratobranchial I continuous with

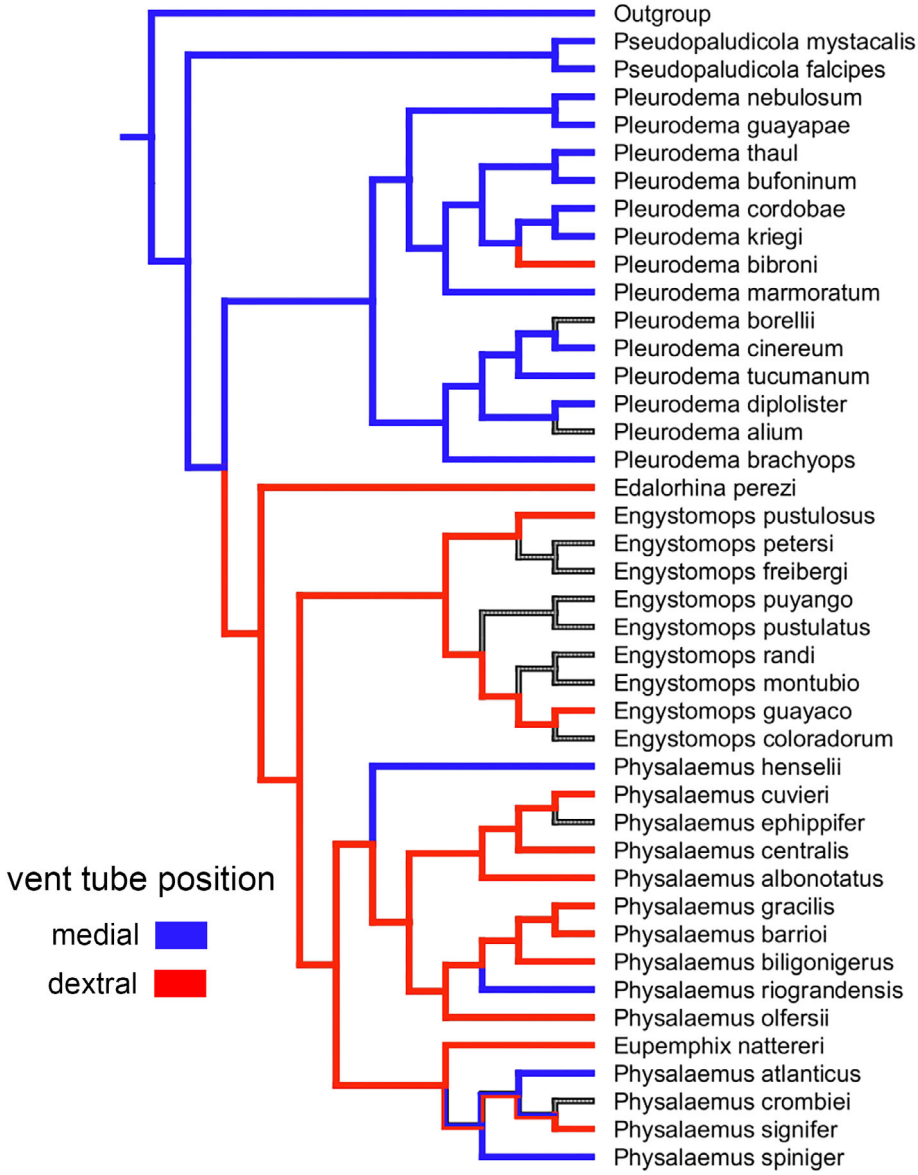

FIGURE 7 Optimization of medial (blue) and dextral (red) vent tube on the topology of the subfamily Leiuperinae from Jetz and Pyron (2018). Branches in grey are those for which the character is unknown for the respective taxa

hypobranchial plates through a strip of cartilage that bears a triangular and medially inclined *processus anterior branchialis*. Ceratobranchials II, III, and IV fused to hypobranchial plates. Ceratobranchials II and III have small processes on their medial margins that are opposite to each other, but are not fused, resulting in an "open" *processus branchialis*. Spicules project dorsally from ceratobranchials I, II, and III on the point of attachment with hypobranchial plates. Spicule IV modified in a cartilage plate on proximal margin of ceratobranchial IV.

3.3.3 | Intraspecific variation

The specimen from Peru (stage 36) differs from the Ecuador samples by presenting a suprarostral cartilage with the corpora separated medially and absence of a ventrolateral connection between each corpus and its respective lateral ala.

4 | DISCUSSION

The only larval information about the genus *Edalorhina* is a brief description of the tadpole of *E. perezi* (Schlüter, 1990). The tadpole of its sister species, *E. nasuta*, remains unknow. Altig and McDiarmid (1999b) provided a descriptive summary of the tadpole external morphology for the genus based on Schlüter (1990) and De la Riva (1995); however, in De la Riva's work there is no mention of *Edalorhina*.

The tadpole described by Schlüter (1990) is overall similar to that provided herein (Table S4), differing mainly in (a) the orientation of the nostril, dorsolaterally in our sample and anterolaterally in the previous work, and (b) in the oral disc position, almost terminal in our specimens and previously reported as ventral and directed anteroventrally. These differences may represent intraspecific variation associated with ontogenetic differences (Schlüter description was based on a specimen in stage 25). Larval characters for some species can be highly variable in early stages of development and tend to stabilize in later stages (usually after stage 32; Grosjean, 2005).

The marginal papillae of the oral disc of *E. perezi* were described as bifurcated ("lips bordered by one row of bifid papillae"; Schlüter, 1990), a rare feature in anurans (Altig & McDiarmid, 1999a). Furthermore, these marginal papillae were also reported as biserial by Altig and McDiarmid (1999b), possibly a reinterpretation of Schlüter's description or illustration. In our samples, the oral discs of *E. perezi* has clearly one row of non-bifid marginal papillae; these papillae may have their bases slightly offset and directed in alternating directions on lower labium, which could be mistaken for bifid papillae.

The phylogenetic relationships of *Edalorhina* and *Physalaemus* (including *Engystomps*) are supported by adult morphology (Duellman & Morales, 1990; Dunn, 1949; Lynch, 1971; Parker, 1927) and recent molecular analyses corroborated this association (Faivovich et al., 2012; Jetz & Pyron, 2018; Lourenço et al., 2015; Pyron & Wiens, 2011; Veiga-Menoncello et al., 2014), recovering a clade consisting of *Edalorhina*, *Physalaemus*, and *Engystomos*. Despite the distinct morphology of adults of *Edalorhina*, for example, lack of vomerine teeth, presence of cranial crests, and elongated papillae on eyelids (Dunn, 1949; Lynch, 1971; Noble, 1931; Parker, 1927), no morphological character has been suggested as synapomorphic for the two species of the genus.

Larval external morphology has been described for four of the nine species of *Engystomops* and for 36 of the 48 known species of *Physalaemus* (Table S4). Tadpoles of those genera plus *Edalorhina* share the overall pattern of a generalized pond morphology, most with depressed bodies, dorsal eyes, oral disc with keratinized mouthparts, LTRF 2/3, low fins with rounded or slightly pointed tip, and dorsal fin originating at or near the body-tail junction; all traits that fit the ecomorphological guild II:A:1 (Altig & Johnston, 1989; McDiarmid & Altig, 1999). *Edalorhina perezi* differs from other species in the clade by having an almost terminal oral disc (ventral to anteroventral in other species). An exception would be *Physalaemus fernandezae*, described as having a "sub-terminal oral disc" (Alcalde, Natale, & Cajade, 2006). However, the larva of this species is readily differentiated from *E. perezi* by having a midventral gap on labium. Moreover, the LTRF 2(2)/3(1) separates *E. perezi* from all described *Physalaemus* larvae in the *P. biligonigerus* group (sensu Lourenço et al., 2015), plus *P. centralis* (P3 labial tooth row absent in these species; Rossa-Feres & Jim, 1993; Fabrezi & Vera, 1997; Perotti & Céspedez, 1999; Nomura, Rossa-Feres, & Prado, 2003; Rossa-Feres & Nonura, 2006; Vera Candioti, 2007; Borteiro & Kolenc, 2007; Schulze, Jansen, & Köhler, 2015). A vent tube with dextral opening is found in *Edalorhina*, *Engystomops*, and most *Physalaemus* (Table S4). Among Leiuperinae, most *Pleurodema* and *Pseudopaludicola* have a medial vent tube (Andrade, Ferreira, Takazone, Libório, & Weber, 2018; Barrasso, Alcalde, Martinazzo, & Basso, 2012; Cei, 1980; Galvani, Gonzalez, Sanabria, & Quiroga, 2012; Kher & Schaefer, 2005; Kolenc et al., 2009; Laufer & Barreneche, 2008; Lobo, 1991; Magalhães, Loebmann, Kokubum, Haddad, & Garda, 2014; Pereira & Nascimento, 2004; Schulze et al., 2015; Toledo, 2010), a character-state also found in most genera of Leptodactylidae (e.g., Almeida & Angulo, 2006; de Sá, Langone, & Segalla, 2007; Grosso, 2015; Heyer & Silverstone, 1969; Lamar & Wild, 1995; Magalhães, Garda, Amado, & de Sá, 2013; Menin, de Almeida, & Kokubum, 2009; Menin, Lima, & Rodrigues, 2010; Mêrces, Magalhaes, Amado, Junca, & Garda, 2015; Rossa-Feres & Nonura, 2006; Schulze et al., 2015; Zaracho & Kokubum, 2017) as well as in many Centrolenidae, the sister group of Leptodactylidae (Jetz & Pyron, 2018; for centrolenids tadpoles, see Rada et al., 2019 and references therein). When we optimize this character on the phylogeny of Leiuperinae provided by Jetz and Pyron (2018), the presence of a dextral vent tube emerge as a synapomorphy of *Edalorhina*, *Engystomops*, and *Physalaemus* (Figure 7).

Larval buccopharyngeal cavity morphology data are largely missing for this clade. Information is available for two species of *Engystomops* (*E. petersi* and *E. pustulosus*; Wassersug & Heyer, 1988) and for about 50% of the known species of *Physalaemus* (25 of the 48 species; Table S5). However, some interesting information emerges from the analysis of the available data. *E. perezi* has a trapezoidal (flap-like) lateral ridge papillae. A flap-like lateral ridge papillae (trapezoidal or triangular) was also reported in *Engystomops* (Table S5) and, within Leuperinae, in *Pleurodema* (Barrasso et al., 2012; Fabrezi & Vera, 1997; Wassersug & Heyer, 1988), differing from the bifurcated or trifurcated (chela-shaped) lateral ridge papillae of most *Physalaemus*

(except in one population of *P. albonotatus* [Miranda & Ferreira, 2009], *P. fernandezae* [Alcalde et al., 2006], and *P. lisei* [Both, Kwet, & Solé, 2006]).

Three characters of the buccal cavity are diagnostic for *E. perezi* and candidates for autapomorphies of *Edalorhina* (i.e., pending on data in *E. nasuta* tadpoles): (a) the presence of two lingual papillae (also found only in *Physalemus marmoratus*, Nomura et al., 2003 and *P. riograndensis*, Sandoval, 2002), (b) a filiform median ridge that is longer than wide, differing from the usual wider than long (trapezoidal, triangular, or semicircular) median ridge in the remaining Leiuperinae, and (c) the buccal roof with no papillae on BRA (other Leiuperinae have a variable number of BRA papillae, that is, 4 to 16; Table S5).

Knowledge on the larval skeleton of the *Edalorhina*, *Engystomops*, and *Physalaemus* clade is still scarce. The chondrocranium of *E. perezi* described in an unpublished Master thesis (Turner, 1999) overall agrees with our analysis. Only five species of *Physalaemus* have available descriptions (Table S6). *E. perezi* differs from *Physalaemus* by the presence of a *processus pseudopterygoideus* and a suprarostral with corpora and alae joined by dorsal and ventral connections (absence of a *processus pseudopterygoideus* and suprarostral with only dorsal connection in *Physalaemus*). Available data for other Leiuperinae showed the presence of a *processus pseudopterygoideus* in *Pseudopaludicola falcipes* (Alcalde & Barrasso, 2013) and *Pleurodema* (Barrasso et al., 2012; Fabrezi & Vera, 1997). However, in *E. perezi* this process has a unique morphology with its medial margin partially fused with the orbital cartilage; differing from the condition reported in most other species that have conical shape and free margins. A suprarostral cartilage with ventral connections between corpora and alae was reported in *Pseudopaludicola canga* and *P. falcipes* (Alcalde & Barrasso, 2013; Andrade et al., 2018), however, the lack of this connection was reported for *P. boliviana* (Alcalde & Barrasso, 2013) and *Pleurodema* (Barrasso et al., 2012; Fabrezi & Vera, 1997). Furthermore, *Edalorhina* larval skeleton differs from *Pleurodema* by the presence of a hyobranchial apparatus with an "open" *processus branchialis* ("closed" in *Pleurodema*, Barrasso et al., 2012).

5 | CONCLUSIONS

The larval morphology of *E. perezi* provides useful systematic information and herein we identified some characters that are diagnostic for the species and putative autapomorphies for the genus *Edalorhina*, such as the presence of two lingual papillae, a filiform median ridge, and the buccal roof with no papillae on BRA, await confirmation in the other known species in the genus (*E. nasuta*) and a comprehensive phylogenetic analysis of the family Leptodacylidae. The skeleton also presents some unique characteristics that readily differentiates from the remaining Leiuperinae, as the presence and peculiar shape of the *processus pseudopterygoideus* and a suprarostral cartilage with corpora and alae joined through dorsal and ventral connections.

ACKNOWLEDGMENTS

We thank Santiago Ron (QCAZ) for loan of the specimens and the Center of Microscopy at the Universidade Federal de Minas Gerais (www.microscopia.ufmg.br) for providing the equipment and technical support for analysis involving electron microscopy. Paulo C. A. Garcia thanks the productivity grant provided by the Conselho Nacional de Desenvolvimento Científico e Tecnológico (CNPq). This study is part of the Doctoral thesis of the first author and was financed in part by the Coordenação de Aperfeiçoamento de Pessoal de Nível Superior - Brasil (CAPES) - Finance Code 001.

AUTHOR CONTRIBUTIONS

Filipe Augusto Nascimento: Conceptualization; formal analysis; investigation; methodology; writing-original draft. **Rafael de Sá:** Conceptualization; methodology; supervision; writing-original draft. **Paulo A. Garcia:** Conceptualization; methodology; supervision; writing-original draft.

PEER REVIEW

The peer review history for this article is available at https://publons.com/publon/10.1002/jmor.21286.

DATA AVAILABILITY STATEMENT

The data that supports the findings of this study are available in the supplementary material of this article.

ORCID

Filipe A. C. do Nascimento https://orcid.org/0000-0002-1684-3753
Rafael O. de Sá https://orcid.org/0000-0002-6137-962X
Paulo C. de A. Garcia https://orcid.org/0000-0002-4789-7033

REFERENCES

Aichinger, M. (1987). Annual activity patterns of anurans in a seasonal neotropical environment. *Oecologia*, *71*, 583–592. https://doi.org/10.1007/BF00379302

Alcalde, L., & Barrasso, D. A. (2013). Internal features of larvae belonging to two species of *Pseudopaludicola* (Anura: Leiuperinae). *Amphibia-Reptilia*, *34*, 129–135. https://doi.org/10.1163/15685381-00002870

Alcalde, L., Candioti, F. V., Kolenc, F., Borteiro, C., & Baldo, D. (2011). Cranial anatomy of tadpoles of five species of *Scinax* (Hylidae, Hylinae). *Zootaxa*, *2787*, 19–36. https://doi.org/10.11646/zootaxa.2787.1.2

Alcalde, L., Natale, G. S., & Cajade, R. (2006). The tadpole of *Physalaemus fernandezae* (Anura: Leptodactylidae). *Herpetological Journal*, *16*, 203–211.

Alcalde, L., & Rosset, S. D. (2003). Descripción y comparación del condrocráneo en larvas de *Hyla raniceps* (Cope, 1862), *Scinax granulatus* (Peters, 1871) y *Scinax squalirostris* (A. Lutz, 1925) (Anura: Hylidae). *Cuadernos de Herpetología*, *17*, 33–49.

Almeida, A. P., & Angulo, A. (2006). A new species of *Leptodactylus* (Anura: Leptodactylidae) from the state of Espírito Santo, Brazil, with remarks on the systematics of associated populations. *Zootaxa*, *1334*, 1–25. https://doi.org/10.11646/zootaxa.1334.1.1

Altig, R., & Johnston, G. F. (1989). Guilds of anuran larvae: Relationships among developmental modes, morphologies, and habits. *Herpetological Monographs*, *3*, 81–109. https://doi.org/10.2307/1466987

Altig, R., & McDiarmid, R. W. (1999a). Body plan. Development and morphology. In R. W. McDiarmid & R. Altig (Eds.), *Tadpoles: The biology of anuran larvae* (pp. 24–51). Chicago: University of Chicago Press.

Altig, R., & McDiarmid, R. W. (1999b). Diversity, familial and generic characterization. In R. W. McDiarmid & R. Altig (Eds.), *Tadpoles: The biology of anuran larvae* (pp. 295–337). Chicago: University of Chicago Press.

Andrade, E. B., Ferreira, J. S., Takazone, A. M., Libório, A. E. C., & Weber, L. N. (2018). Description of the tadpole of *Pseudopaludicola canga* Giaretta and Kokubum, 2003 (Anura: Leptodactylidae). *South American Journal of Herpetology*, *13*, 64–72. https://doi.org/10.2994/SAJH-D-17-00032.1

Barrasso, D. A., Alcalde, L., Martinazzo, L. B., & Basso, N. G. (2012). External morphology, chondrocranium, cranial muscles, and buccopharyngeal features of tadpoles of *Pleurodema thaul* (Anura: Leiuperidae): A comparison with *P. bufoninum*. *Herpetologica*, *68*, 48–59. https://doi.org/10.1655/HERPETOLOGICA-D-11-00028.1

Barrasso, D. A., Cotichelli, L., Alcalde, L., & Basso, N. G. (2013). Redescription of the tadpole of *Pleurodema somuncurensis* (Cei, 1969) (Amphibia: Anura). *Zootaxa*, *3681*, 192–196. https://doi.org/10.11646/zootaxa.3681.2.10

Barrio, A. (1954). Sistemática, morfología y reproduccion de *Physalaemus henselii* (Peters) y *Pseudopaludicola falcipes* (Hensel). *Physis*, *20*, 379–389.

Borteiro, C., & Kolenc, F. (2007). Redescription of the tadpoles of three species of frogs from Uruguay (Amphibia: Anura: Leiuperidae and Leptodactylidae), with notes on natural history. *Zootaxa*, *1638*, 1–20. https://doi.org/10.11646/zootaxa.1638.1.1

Both, C., Kwet, A., & Solé, M. (2006). The tadpole of *Physalaemus lisei* Braun and Braun, 1977 (Anura, Leptodactylidae) from southern Brazil. *Alytes*, *24*, 109–116.

Cannatella, D. (1999). Architecture. Cranial and axial musculoskeleton. In R. W. McDiarmid & R. Altig (Eds.), *Tadpoles: The biology of anuran larvae* (pp. 52–991). Chicago: University of Chicago Press.

Cei, J. M. (1980). Amphibians of Argentina. *Monitore Zoologico Italiano*. *Nueva Serie*, *Monographia*, *2*, 1–609.

De La Riva, I. (1995). A new reproductive mode for the genus *Adenomera* (Amphibia: Anura: Leptodactylidae): Taxonomic implications for certain Bolivian and Paraguayan populations. *Studies on Neotropical Fauna and Environment*, *30*, 15–29. https://doi.org/10.1080/01650529509360937

de Sá, R. O., Langone, J. A., & Segalla, M. V. (2007). The tadpole of *Leptodactylus notoaktites* Heyer, 1978 (Anura, Leptodactylidae). *South American Journal of Herpetology*, *2*, 69–75. https://doi.org/10.2994/1808-9798(2007)2[69:TTOLNH]2.0.CO;2

Dingerkus, G., & Uhler, L. D. (1977). Enzyme clearing of alcian blue stained whole small vertebrates for demonstration of cartilage. *Stain Technology*, *52*, 229–232. https://doi.org/10.3109/10520297709116780

Duellman, W. E., & Morales, V. R. (1990). Variation, distribution, and life history of *Edalorhina perezi* (Amphibia, Anura, Leptodactylidae). *Studies on Neotropical Fauna and Environment*, *25*, 19–30. https://doi.org/10.1080/01650529009360798

Dunn, E. R. (1949). Notes on the south American frog genus *Edalorhina*. *American Museum Novitates*, *1416*, 1–10.

Fabrezi, M., & Vera, R. (1997). Caracterización morfológica de larvas de anuros del noroeste argentino. *Cuadernos de Herpetología*, *11*, 37–49.

Faivovich, J., Ferraro, D. P., Basso, N. G., Haddad, C. F. B., Rodrigues, M. T., Wheeler, W. C., & Lavilla, E. O. (2012). A phylogenetic analysis of *Pleurodema* (Anura: Leptodactylidae: Leiuperinae) based on mitochondrial and nuclear gene sequences, with comments on the evolution of anuran foam nests. *Cladistics*, *28*, 460–482. https://doi.org/10.1111/j.1096-0031.2012.00406.x

Frost, D. R. (2019). *Amphibian species of the world: An online reference. Version 6.0*. New York, USA: American Museum of Natural History. http://research.amnh.org/herpetology/amphibia/index.html

Galvani, G., Gonzalez, E., Sanabria, E., & Quiroga, L. (2012). The tadpole of *Pleurodema nebulosum* Burmeister (Anura: Leiuperidae). *Zootaxa*, *3450*, 9–11. https://doi.org/10.11646/zootaxa.3450.1.3

Giaretta, A. A., & Facure, K. G. (2009). Habitat, egg-laying behaviour, eggs and tadpoles of four sympatric species of *Pseudopaludicola* (Anura, Leiuperidae). *Journal of Natural History*, *43*, 995–1009. https://doi.org/10.1080/00222930802702456

Gosner, K. L. (1960). A simplified table for staging anuran embryos and larvae with notes on identification. *Herpetologica*, *16*, 183–190.

Grosjean, S. (2005). The choice of external morphological characters and developmental stages for tadpole-based anuran taxonomy: A case study in *Rana* (*Sylvirana*) *nigrovittata* (Blyth, 1855) (Amphibia, Anura, Ranidae). *Contributions to Zoology*, *74*, 61–76. https://doi.org/10.1163/18759866-0740102005

Grosso, J. R. (2015). Tadpole morphology of *Leptodactylus plaumanni* (Anura: Leptodactylidae), with comments on the phylogenetic significance of larval characters in *Leptodactylus*. *Cuadernos de Herpetología*, *29*, 117–129.

Haas, A. (2003). Phylogeny of frogs as inferred from primarily larval characters (Amphibia, Anura). *Cladistics*, *19*, 23–89. https://doi.org/10.1016/S0748-3007(03)00006-9

Heyer, W. R., & Silverstone, P. A. (1969). The larva of the frog *Leptodactylus hylaedactylus* (Leptodactylidae). *Fieldiana Zoology*, *51*, 141–145. https://doi.org/10.5962/bhl.title.3047

Jetz, W., & Pyron, R. A. (2018). The interplay of past diversification and evolutionary isolation with present imperilment across the amphibian tree of life. *Nature Ecology & Evolution*, *2*, 850–858. https://doi.org/10.1038/s41559-018-0515-5

Kher, A. I., & Schaefer, E. F. (2005). Description of the tadpole of *Pseudopaludicola boliviana* (Anura: Leptodactylidae). *Herpetological Review*, *36*, 250–251.

Kohler, G. (2012). Color catalogue for field biologist. Offenbach: Herpeton.

Kolenc, F., Borteiro, C., Baldo, D., Ferraro, D., & Prigioni, C. (2009). The tadpoles and advertisement calls of *Pleurodema bibroni* Tschudi and *Pleurodema kriegi* (Müller), with notes on their geographic distribution and conservation status (Amphibia, Anura, Leiuperidae). *Zootaxa*, *1969*, 1–35. https://doi.org/10.11646/zootaxa.1969.1.1

Lamar, W. W., & Wild, E. R. (1995). Comments on the natural history of *Lithodytes lineatus* (Anura: Leptodactylidae), with description of the tadpole. *Herpetological Natural History*, *3*, 135–142.

Larson, P. M., & de Sá, R. O. (1998). Chondrocranium morphology of *Leptodactylus* larvae (Leptodactylidae; Leptodactylinae): Its utility in phylogenetic reconstruction. *Journal of Morphology*, *238*, 287–305. https://doi.org/10.1002/(SICI)1097-4687(199812)238:3<287::AID-JMOR2>3.0.CO;2-8

Laufer, G., & Barreneche, J. M. (2008). Re-description of the tadpole of *Pseudopaludicola falcipes* (Anura: Leiuperidae), with comments on larval diversity of the genus. *Zootaxa*, *1760*, 50–58. https://doi.org/10.11646/zootaxa.1760.1.4

Lavilla, E. O., & Scrocchi, G. J. (1986). Morfometría larval de los géneros de Telmatobiinae (Anura: Leptodactylidae) de Argentina y Chile. *Physis*, *44*, 39–43.

Lobo, F. (1991). Descripción de la larva de *Pseudopaludicola mystacalis* (Anura: Leptodactylidae). *Boletín de la Asociación Herpetológica Argentina*, *7*, 22–24.

Lourenço, L. B., Targueta, C. P., Baldo, D., Nascimento, J., Garcia, P. C., Andrade, G. V., … Recco-Pimentel, S. M. (2015). Phylogeny of frogs from the genus *Physalaemus* (Anura, Leptodactylidae) inferred from mitochondrial and nuclear gene sequences. *Molecular Phylogenetics and Evolution*, *92*, 204–216. https://doi.org/10.1016/j.ympev.2015.06.011

Lynch, J. D. (1971). Evolutionary relationships, osteology, and zoogeography of leptodactyloid frogs. *Miscellaneous Publications of the Museum of Natural History of the University of Kansas*, *53*, 1–238.

Maddison, W.P. & Maddison, D.R. (2016). Mesquite: a modular system for evolutionary analysis (ver. 3.20) [Computer software]. www.mesquiteproject.org

Magalhães, F. M., Garda, A. A., Amado, T. F., & de Sá, R. O. (2013). The tadpole of *Leptodactylus caatingae* Heyer and Juncá, 2003 (Anura: Leptodactylidae): External morphology, internal anatomy, and natural history. *South American Journal of Herpetology*, *8*, 203–210. https://doi.org/10.2994/SAJH-D-13-00033.1

Magalhães, F. M., Loebmann, D., Kokubum, M. N. C., Haddad, C. F. B., & Garda, A. A. (2014). A new species of *Pseudopaludicola* (Anura:

Leptodactylidae: Leiuperinae) from northeastern Brazil. *Herpetologica*, *70*, 77–88. https://doi.org/10.1655/HERPETOLOGICA-D-13-00054

McDiarmid, R. W., & Altig, R. (1999). Research: Materials and techniques. In R. W. McDiarmid & R. Altig (Eds.), *Tadpoles. The biology of anuran larvae* (pp. 7–23). Chicago: University of Chicago Press.

Menin, M., de Almeida, A. P., & Kokubum, M. N. C. (2009). Reproductive aspects of *Leptodactytus hylaedactylus* (Anura: Leptodactylidae), a member of the *Leptodactylus marmoratus* species group, with a description of tadpoles and calls. *Journal of Natural History*, *43*, 2257–2270. https://doi.org/10.1080/00222930903097707

Menin, M., Lima, A. P., & Rodrigues, D. J. (2010). The tadpole of *Leptodactylus pentadactylus* (Anura: Leptodactylidae) from Central Amazonia. *Zootaxa*, *2508*, 65–68. https://doi.org/10.11646/zootaxa.2508.1.5

Mêrces, E. D. A., Magalhaes, F. D. M., Amado, T. F., Junca, F. A., & Garda, A. A. (2015). Tadpole of *Leptodactylus oreomantis* Carvalho, Leite and Pezzuti 2013 (Anura, Leptodactylidae). *Zootaxa*, *3911*, 589–592. https://doi.org/10.11646/zootaxa.3911.4.8

Miranda, N. E. O., & Ferreira, A. (2009). Morfologia oral interna de larvas dos gêneros *Eupemphix*, *Physalaemus* e *Leptodactylus* (Amphibia: Anura). *Biota Neotropica*, *9*, 165–176. https://doi.org/10.1590/S1676-06032009000200016

Noble G. K. (1931). *The Biology of the Amphibia*. McGraw-Hill. https://doi.org/10.5962/bhl.title.82448.

Nomura, F., Rossa-Feres, D. C., & Prado, V. H. M. (2003). The tadpole of *Physalaemus fuscomaculatus* (Anura: Leptodactylidae), with a description of internal oral morphology. *Zootaxa*, *370*, 1–8. https://doi.org/10.11646/zootaxa.370.1.1

Parker, H. W. (1927). A revision of the frogs of the genera *Pseudopaludicola*. *Physalaemus and Pleurodema*. *Annals and Magazine of Natural History*, *6*, 450–478. https://doi.org/10.1080/00222932708655471

Pereira, E. G., & Nascimento, L. B. (2004). Descrição da vocalização e do girino de *Pseudopaludicola* mineira Lobo, 1994, com notas sobre a morfologia de adultos (Amphibia, Anura, Leptodactylidae). *Arquivos Do Museu Nacional Do Rio de Janeiro*, *62*, 233–240.

Perotti, M. G., & Céspedez, J. A. (1999). The tadpole of *Physalaemus santafecinus*, with comments on the buccoharyngeal morphology. *Journal of Herpetology*, *33*, 312–315. https://doi.org/10.2307/1565731

Pinheiro, P. D. P., Pezzuti, T. L., & Garcia, P. C. D. A. (2012). The tadpole and vocalizations of *Hypsiboas polytaenius* (Cope, 1870) (Anura, Hylidae, Hylinae). *South American Journal of Herpetology*, *7*, 123–133. https://doi.org/10.2994/057.007.0202

Pyron, A. R., & Wiens, J. J. (2011). A large-scale phylogeny of amphibian including over 2800 species, and a revised classification of extant frogs, salamanders, and cecilians. *Molecular Phylogenetics and Evolution*, *61*, 543–583. https://doi.org/10.1016/j.ympev.2011.06.012

Rada, M., Dias, P. H. D. S., Pérez-Gonzalez, J. L., Anganoy-Criollo, M., Rueda-Solano, L. A., Pinto-E, M. A., … Grant, T. (2019). The poverty of adult morphology: Bioacoustics, genetics, and internal tadpole morphology reveal a new species of glassfrog (Anura: Centrolenidae: Ikakogi) from the Sierra Nevada de Santa Marta, Colombia. *PLoS One*, *14*, 1–46.

Rasband, W. S. (1997-2018). *ImageJ*, Maryland: National Institutes of Health. https://imagej.nih.gov/ij/.

Ron, S. R., Coloma, L. A., & Cannatella, D. C. (2005). A new cryptic species of *Physalaemus* (Anura: Leptodactylidae) from western Ecuador with comments on the call structure of the *P. pustulosus* species group. *Herpetologica*, *61*, 178–198. https://doi.org/10.1655/04-38

Rossa-Feres, D. C., & Nonura, F. (2006). Characterization and taxonomic key for tadpoles (Amphibia: Anura) from the northwestern region of São Paulo state, Brazil. *Biota Neotropica*, *6*, 1–26. https://doi.org/10.1590/S1676-06032006000100014

Rossa-Feres, D. D. C., & Jim, J. (1993). Tadpole of *Physalaemus centralis* (Anura, Leptodactylidae). *Copeia*, *1993*, 566–569. https://doi.org/10.2307/1447165

Ruggeri, J., & Weber, L. N. (2012). A survey of the internal oral features and external morphology of *Physalaemus* larvae (Anura, Leptodactylidae). *Zootaxa*, *3200*, 1–26. https://doi.org/10.11646/zootaxa.3200.1.1

Sandoval, M. T. (2002). Descripción del disco oral y de la cavidad bucofaríngea de larvas de dos especies de anuros de la familia Leptodactylidae. Reunión de Comunicaciones científicas de la UNN, 1–3.

Schlüter, A. (1990). Reproduction and tadpole of *Edalorhina perezi* (Amphibia, Leptodactylidae). *Studies on Neotropical Fauna and Environment*, *25*, 49–56. https://doi.org/10.1080/01650529009360801

Schulze, A., Jansen, M., & Köhler, G. (2015). Tadpole diversity of Bolivia's lowland anuran communities: Molecular identification, morphological characterization, and ecological assignment. *Zootaxa*, *4016*, 1–111. https://doi.org/10.11646/zootaxa.4016.1.1

Toledo, L. F. (2010). Description of a new species of *Pseudopaludicola* Miranda-Ribeiro, 1926 from the state of São Paulo, southeastern Brazil (Anura, Leiuperidae). *Zootaxa*, *2681*, 47–56. https://doi.org/10.11646/zootaxa.2681.1.4

Turner, W. (1999). *Evolution of the chondrocranium in Leptodactylidae* (M. Sc. Thesis), Univeristy of Richmod, Richmond, VA.

Veiga-Menoncello, A. C. P., Lourenço, L. B., Strussmann, C., Rossa-Feres, D. C., Andrade, G. V., Giaretta, A. A., & Recco-Pimentel, S. M. (2014). A phylogenetic analysis of *Pseudopaludicola* (Anura) providing evidence of progressive chromosome reduction. *Zoologica Scripta*, *43*, 261–272. https://doi.org/10.1111/zsc.12048

Vera Candioti, M. F. (2007). Anatomy of anuran tadpoles from lentic water bodies: Systematic relevance and correlation with feeding habits. *Zootaxa*, *1600*, 1–175.

Vera Candioti, M. F., Haad, B., Baldo, D., Kolenc, F., Borteiro, C., & Altig, R. (2011). Different pathways are involved in the early development of the transient oral apparatus in anuran tadpoles (Anura: Leiuperidae). *Biological Journal of the Linnean Society*, *104*, 330–345. https://doi.org/10.1111/j.1095-8312.2011.01727.x

Wassersug, R. J. (1976). Oral morphology of anuran larvae: Terminology and general description. Occasional Papers of the Museum of Natural History, University of Kansas, *48*, 1–23.

Wassersug, R. J. (1980). Internal oral features of eight anuran families: Functional, systematic, evolutionary and ecological considerations. Miscellaneous Publications, Museum of Natural History of the University of Kansas, *68*, 1–146. https://doi.org/10.5962/bhl.title.16230

Wassersug, R. J., & Heyer, W. R. (1988). A survey of internal oral features of Leptodactyloid larvae (Amphibia: Anura). *Smithsonian Contributions to Zoology*, *457*, 1–97. https://doi.org/10.5479/si.00810282.457

Weigandt, M., Úbeda, C. A., & Díaz, M. (2004). The larva of *Pleurodema bufoninum* Bell, 1843, with comments on its biology and on the egg strings (Anura, Leptodactylidae). *Amphibia-Reptilia*, *25*, 429–437.

Zaracho, V. H., & Kokubum, M. N. C. (2017). Reproduction and larval morphology of *Adenomera diptyx* (Anura: Leptodactylidae) from the Argentinean humid Chaco and Brazilian pantanal. *Salamandra*, *53*, 1–9.

SUPPORTING INFORMATION

Additional supporting information may be found online in the Supporting Information section at the end of this article.

How to cite this article: do Nascimento FAC, de Sá RO, de A. Garcia PC. Tadpole of the Amazonia frog *Edalorhina perezi* (Anura: Leptodactylidae) with description of oral internal and chondrocranial morphology. *Journal of Morphology*. 2021;282: 115–126. https://doi.org/10.1002/jmor.21286